

Testing Color Evaporation in Photon-Photon Production of J/ψ at CERN LEP II

O. J. P. Éboli,^{1,*} E. M. Gregores,^{2,†} and J. K. Mizukoshi^{1,‡}

¹*Instituto de Física, Universidade de São Paulo, São Paulo – SP, Brazil.*

²*Instituto de Física Teórica, Universidade Estadual Paulista, São Paulo – SP, Brazil.*

Abstract

The DELPHI Collaboration has recently reported the measurement of J/ψ production in photon-photon collisions at LEP II. These newly available data provide an additional proof of the importance of colored $c\bar{c}$ pairs for the production of charmonium because these data can only be explained by considering resolved photon processes. We show here that the inclusion of color octet contributions to the J/ψ production in the framework of the color evaporation model is able to reproduce this data. In particular, the transverse-momentum distribution of the J/ψ mesons is well described by this model.

PACS numbers: 13.60.Le, 14.40.Gx

*Electronic address: eboli@fma.if.usp.br

†Electronic address: gregores@ift.unesp.br

‡Electronic address: mizuka@fma.if.usp.br

I. INTRODUCTION

DELPHI Collaboration recently released preliminary measurements of the transverse momentum spectrum of J/ψ mesons produced in $\gamma\gamma$ collisions at LEP [1, 2]. This new data allow further tests of models for charmonium production. We show here that the Color Evaporation Model (CEM) reproduces these new results using the same single non-perturbative parameter that has been obtained from previous analysis of charmonium photo- and hadro-production. These newly available data provide an additional proof of the importance of colored $c\bar{c}$ pairs for the production of charmonium, as the data on this region can only be explained by considering resolved photon processes, which forms colored $c\bar{c}$ pairs in the leading order. The CEM for charmonium production incorporates these colored pairs into the total yield of charmonium in a very simple and economical way.

The Tevatron data [3, 4] on charmonium production at high p_T changed the way we understand charmonium production. The presently successful models are based in two key considerations: i) onium production is a two-step process where a heavy quark pair is produced first, followed by the non-perturbative formation of the asymptotic states, and ii) color octet as well as singlet $c\bar{c}$ states contribute to the production of charmonia. These features are incorporated in the Non-Relativistic QCD (NRQCD) factorization approach [5, 6], in the Color Evaporation Model [7, 8, 9], and in the Soft Color Interaction Model [10].

The Color Evaporation Model simply states that charmonium production is described by the same dynamics as $D\bar{D}$ production, *i.e.*, by the formation of a $c\bar{c}$ pair in any color configuration. Rather than imposing that the $c\bar{c}$ pair is in a color singlet state in the short distance perturbative processes, it is argued that the appearance of color singlet asymptotic states solely depends on the outcome of non-perturbative large distance fluctuations of quarks and gluons. These large distance fluctuations are considered to be complex enough for the occupation of different color states to approximately respect statistical counting. In fact, it is indeed hard to imagine that a color singlet state formed at a range m_ψ^{-1} would survive to form a ψ at a range Λ_{QCD}^{-1} . Although far more restrictive than other proposals, CEM successfully accommodates all features of charmonium production [11, 12, 13].

The CEM predicts that the sum of the production cross sections of all onium and open charm states is described by

$$\sigma_{\text{onium}} = \frac{1}{9} \int_{2m_c}^{2m_D} dM_{c\bar{c}} \frac{d\sigma_{c\bar{c}}}{dM_{c\bar{c}}}, \quad (1)$$

and

$$\sigma_{\text{open}} = \frac{8}{9} \int_{2m_c}^{2m_D} dM_{c\bar{c}} \frac{d\sigma_{c\bar{c}}}{dM_{c\bar{c}}} + \int_{2m_D} dM_{c\bar{c}} \frac{d\sigma_{c\bar{c}}}{dM_{c\bar{c}}} , \quad (2)$$

where $M_{c\bar{c}}$ is the invariant mass of the $c\bar{c}$ pair. The factor $1/9$ stands for the probability that a pair of charm quarks formed at a typical time scale $1/M_\psi$ ends up as a color singlet state after exchanging an uncountable number of soft gluons with the reaction remnants; for further details see [7]. One attractive feature of this model is the relation between the production of charmonium and open charm, which allows us to use the open charm data to normalize the perturbative QCD calculation, and consequently to constrain the CEM predictions.

Up to this point, the model has no free parameter in addition to the usual QCD ones. In order to predict the production rate of a particular charmonium state, let us say a J/ψ meson, we must also know the fraction ρ_ψ of produced onium states that materialize as this state (J/ψ),

$$\sigma_\psi = \rho_\psi \sigma_{\text{onium}} . \quad (3)$$

In its simplest version, the CEM assumes that ρ_ψ is energy and process independent, which is in agreement with the low energy measurements [14, 15]. Notice that ρ_ψ is the solely free parameter of the CEM, making this a very restrictive framework. From the charmonium photo-production, we determined that $\rho_\psi = 0.43\text{--}0.5$ [8], a value that can be accounted for by statistical counting of final states [10]. The fact that all ψ production data are described in terms of this single parameter, fixed by J/ψ photo-production, leads to parameter free predictions for Z -boson decay rate into ψ [16], and to charmonium production cross section at Tevatron [17] and HERA [18, 19], as well as in neutrino initiated reactions [20].

II. RESULTS

The differential cross section for the inclusive process $e^+e^- \rightarrow e^+e^-\gamma\gamma \rightarrow J/\psi X$ is

$$\frac{d^2\sigma}{dp_T^2} = \sum_{A,B} \iiint dy^+ dy^- dx_A dx_B f_{\gamma/e^+}(y^+) f_{\gamma/e^-}(y^-) F_{A/\gamma}(x_A) F_{B/\gamma}(x_B) \frac{d^2\hat{\sigma}(AB \rightarrow \psi Y)}{dp_T^2} , \quad (4)$$

where f_{γ/e^\pm} is the bremsstrahlung photon distribution from an electron/positron. We denoted the parton distribution function of the photon by $F_{A[B]/\gamma}(x_{A[B]})$, where $x_{A[B]}$ is the

fraction of the photon momentum carried by the parton $A[B]$. For direct photon interactions ($A[B] \equiv \gamma$), we have $F_{A[B]/\gamma}(x_{A[B]}) = \delta(x_{A[B]} - 1)$. We considered an average electron-positron center-of-mass energy $2E_e = 197$ GeV. We also applied the experimental J/ψ rapidity cut $-2 < \eta_\psi < 2$, and imposed that the $\gamma\gamma$ center-of-mass energy satisfies $W_{\gamma\gamma} < 35$ GeV, where $W_{\gamma\gamma} = 2E_e\sqrt{y^+y^-}$.

In our calculation, we employed the Weizäcker-Williams approximation for the photon distribution

$$f_{\gamma/e^\pm}(y) = \frac{\alpha_{em}}{2\pi} \left[\frac{1 + (1-y)^2}{y} \log\left(\frac{Q_{max}^2}{Q_{min}^2}\right) + 2m_e^2 y \left(\frac{1}{Q_{max}^2} - \frac{1}{Q_{min}^2} \right) \right], \quad (5)$$

with $Q_{min}^2 = m_e^2 y^2 / (1-y)$, and $Q_{max}^2 = (E_e \theta)^2 (1-y) + Q_{min}^2$. Here, the fraction of the parent e^\pm energy (E_e) carried by the photons is $y (= E_\gamma/E_e)$, and θ is the angular cut that guarantees that the photons are real. We used $\theta = 0.032$ radians, as determined by the experiment.

The inclusive subprocess cross section $\hat{\sigma}(AB \rightarrow \psi Y)$ was calculated using the CEM; see Eqs. (1) and (3). The partonic subprocesses contributing to J/ψ production are depicted in the Table I. Notice that both direct and resolved photons contribute to charmonium production in the CEM. We evaluated numerically the tree level helicity amplitudes of the subprocesses displayed in Table I using MADGRAPH [21] and HELAS [22] packages. The adaptative Monte Carlo program VEGAS [23] was employed to perform the phase space integration.

In the framework of the CEM, the evaluation of the photon-photon production cross section contains only the free parameters appearing in the perturbative QCD calculation of the subprocesses presented in Table I, since the CEM free parameter ρ_ψ can be fixed at the value extracted from the photo-production of J/ψ , *i.e.* $\rho_\psi = 0.5$ [8]. We used the leading

Direct	Once Resolved	Twice Resolved
$\gamma\gamma \rightarrow c\bar{c}g$	$\gamma q(\bar{q}) \rightarrow c\bar{c}q(\bar{q})$	$q\bar{q} \rightarrow c\bar{c}g$
	$\gamma g \rightarrow c\bar{c}g$	$gq(\bar{q}) \rightarrow c\bar{c}q(\bar{q})$
		$gg \rightarrow c\bar{c}g$

TABLE I: Subprocesses contributing to J/ψ production in $\gamma\gamma$ collisions. Here q stands for the light quark flavors u, d, s .

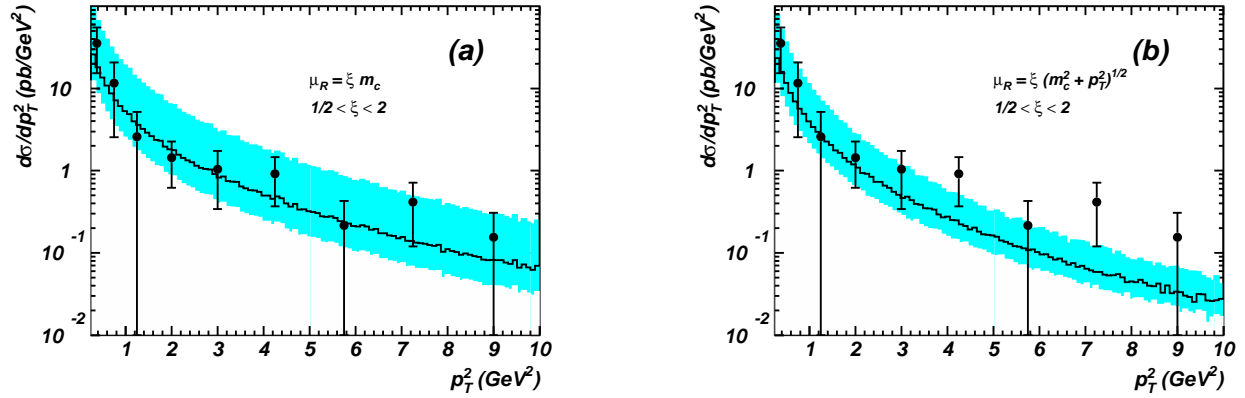


FIG. 1: Uncertainty on the p_T^2 differential cross section originated from different choices of the renormalization scale μ_R . In (a) we chose $\mu_R = \xi m_c$ while in (b) $\mu_R = \xi \sqrt{m_c^2 + p_T^2}$. The shaded band was obtained by varying $\frac{1}{2} < \xi < 2$. We fixed $m_c = 1.3$ GeV, and used the GRS-G parton density function in both figures.

order GRV-G [24] and GRS-G [25] parton density functions as provided by CERN PDFLIB package with the partonic subprocess center-of-mass energy as factorization scale $\mu_F = \sqrt{\hat{s}}$. We verified that our predictions do not vary significantly for other choices of the factorization scales, *e.g.* $\mu_F = \frac{1}{2} \sqrt{\hat{s}}$ and $\mu_F = 2 \sqrt{\hat{s}}$. We also verified that the results are very similar for the GRV-G and GRS-G parton distributions (see Table II). The strong coupling constant was evolved in leading order considering four active flavors and $\Lambda_{QCD}^{(4)} = 300$ MeV, while the charm quark mass was varied between 1.2 and 1.4 GeV.

In order to access the theoretical uncertainties in the lowest order CEM calculations, we analyzed the predicted J/ψ transverse momentum spectrum for different choices of the renormalization scale (μ_R). We present in Fig. 1a the predicted p_T^2 spectrum obtained for $\mu_R = \xi m_c$ with $\frac{1}{2} < \xi < 2$ and $m_c = 1.3$ GeV, as well as the DELPHI experimental results [1, 26]. We can see from this figure that CEM describes well the shape of the distribution, despite the large uncertainty in the absolute value of the differential cross section. Notice that we are only changing a global factor (α_S) for this choice of μ_R when we vary ξ . Figure 1b displays the p_T^2 spectrum for $\mu_R = \xi \sqrt{m_c^2 + p_T^2}$ with $\frac{1}{2} < \xi < 2$ and $m_c = 1.3$ GeV. For this choice of μ_R the uncertainties in the p_T^2 distribution are smaller than for the previous choice of μ_R . However, the shape of the p_T^2 spectrum changes and the CEM prediction seems to diminish faster at large p_T^2 than the data.

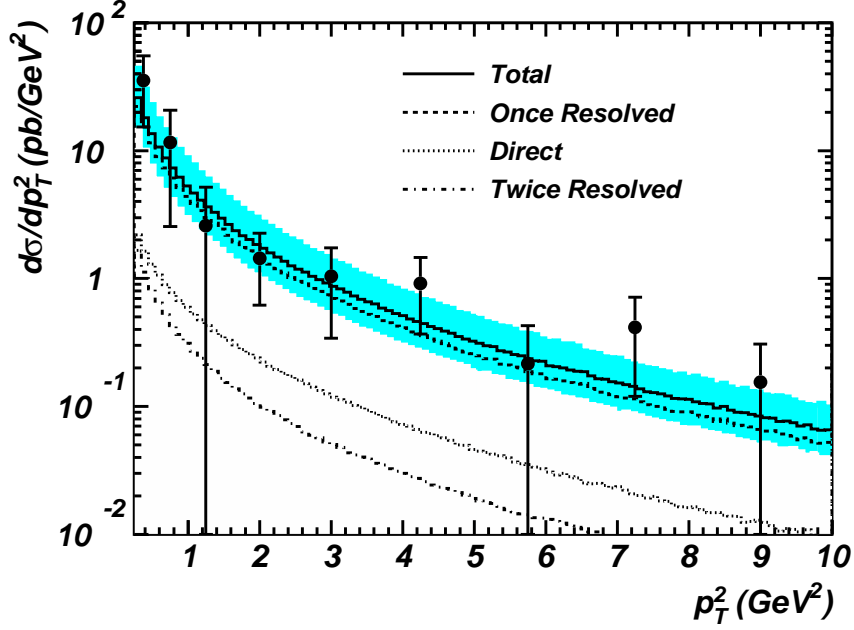


FIG. 2: Differential cross section as function of the squared transverse momentum of the J/ψ . The shaded band shows the theoretical prediction obtained by varying the charm mass ($m_c = 1.3 \pm 0.1$ GeV). We explicitly show the contributions from direct, once resolved and twice resolved cross sections for $m_c = 1.3$ GeV.

In Figure 2 we display the contributions to the J/ψ p_T^2 spectrum arising from direct, once resolved, and twice resolved processes. These distributions were obtained using the GRS-G photon parton densities, $\mu_R = m_c$ and $m_c = 1.3$ GeV. As we can see, the once resolved processes are responsible for the majority of the events ($\simeq 85\%$) while direct and twice resolved processes account for less than 15% of the total cross section. The most important process is $\gamma g \rightarrow c\bar{c}g$. We also present in this figure the uncertainties associated to the charm quark mass; the shaded band represents the sum of all contributions taking $m_c = 1.3 \pm 0.1$ GeV. Notice that the largest uncertainties in the CEM prediction originates from the choice of the renormalization scale. This is quite expected since we are performing our calculation in lowest-order perturbative QCD. We summarize our results for the total cross section in Table II.

In order to further compare our results with the recently published DELPHI results [2, 26], we evaluated the dependence of the total J/ψ yield on the minimum transverse momentum for $\sqrt{s} = 197$ GeV. The result is presented in Fig. 3a. As can be seen from this figure, the

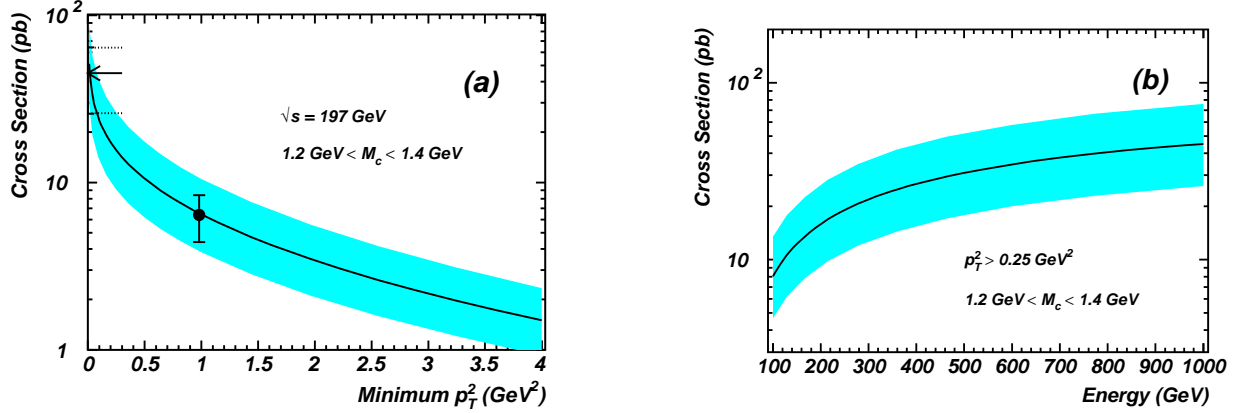


FIG. 3: Total cross section as function of the minimum squared transverse momentum (a) and the e^+e^- center-of-mass energy (b). In (a) the solid line stands for the DELPHI measured total cross section while the dotted lines indicate the experimental error of this quantity. We varied the charm quark mass as $m_c = 1.3 \pm 0.1$ GeV to estimate the theoretical uncertainties. We used $\sqrt{s} = 197$ GeV for the minimum transverse momentum dependence (a) and imposed $p_T^2 > 0.25$ GeV² for the center-of-mass energy dependence (b). The remaining parameters are the same as for Figure 2.

choice of QCD parameters we used in this analysis provides a very good description of the existing data, reinforcing our confidence on the predictive power of the color evaporation model. Figure 3b displays the CEM predictions for the J/ψ production cross section as a function of the e^+e^- center-of-mass energy (\sqrt{s}). Here we assumed that $p_T^2 > 0.25$ GeV², $\mu_R = m_c$ with $m_c = 1.3 \pm 0.1$ GeV, and we used the GRS-G set of parton distribution functions. As expected, the total cross section grows with the center-of-mass energy due to the increase in the photon-photon luminosity. We verified that contributions of direct, once resolved and twice resolved processes are in the same proportion of the results presented for $\sqrt{s} = 197$ GeV; see Fig. 2. Taking into account the planned luminosity of the future e^+e^- colliders, we can easily foresee that it will be possible to extract very precise data on the photon-photon charmonium production in these machines.

III. CONCLUSION

In this paper we showed that the Color Evaporation Model for quarkonium production correctly describes DELPHI data on J/ψ via photon-photon collisions. Due to the rather

Parameters				Cross Sections (pb)			
PDF	m_c	ξ	β	Direct	Once Resolved	Twice Resolved	Total
GRV-G	1.3	1.0	0	1.72	13.3	1.00	16.1
GRS-G	1.3	1.0	0	1.72	13.0	0.94	15.7
GRS-G	1.2	1.0	0	2.75	21.8	1.73	26.3
GRS-G	1.4	1.0	0	1.02	7.5	0.51	9.07
GRS-G	1.3	0.5	0	3.26	46.8	6.42	56.4
GRS-G	1.3	0.5	1	2.42	28.4	3.15	34.0
GRS-G	1.3	1.0	1	1.44	9.65	0.61	11.7
GRS-G	1.3	2.0	0	1.17	5.99	0.29	7.45
GRS-G	1.3	2.0	1	1.03	4.84	0.22	6.08

TABLE II: Cross sections for direct, once resolved, and twice resolved production processes for $p_T^2 > 0.25 \text{ GeV}^2$ using different sets of parton distribution functions, charm masses, and renormalization scales $\mu_R = \xi \sqrt{m_c^2 + \beta p_T^2}$.

large uncertainties in the data, its is not possible to use them to discriminate between the different proposed mechanisms for charmonium production. As far as the DELPHI data are considered, the NRQCD [26] and CEM frameworks present equivalent results.

Considering that the CEM is also successful in describing the photo- and hadro-production of charmonium, we conclude that this model gives a robust and simple parameterization of all charmonium physics. Moreover, $\gamma\gamma$ reactions provide a clear proof of the importance of colored $c\bar{c}$ pairs to the production of charmonium, since the data on this reaction can only be explained considering resolved photon processes, which lead to colored $c\bar{c}$ pairs.

Acknowledgments

This research was supported in part by Fundação de Amparo à Pesquisa do Estado de São Paulo (FAPESP), by Conselho Nacional de Desenvolvimento Científico e Tecnológico

(CNPq), and by Programa de Apoio a Núcleos de Excelência (PRONEX).

- [1] S. Todorova-Nova, *Proceedings of the 31st International Symposium on Multiparticle Dynamics (ISMD 2001)*, Datong, China, 2001.
- [2] J. Abdallah *et al.* [DELPHI Collaboration], Phys. Lett. B **565**, 76 (2003).
- [3] F. Abe *et al.* [CDF Collaboration], Phys. Rev. Lett. **69**, 3704 (1992); *ibid* **79**, 572 (1997); *ibid* **79**, 578 (1997).
- [4] S. Abachi *et al.* [DØ Collaboration], Phys. Lett. B **370**, 239 (1996).
- [5] G. T. Bodwin, E. Braaten, and G. P. Lepage, Phys. Rev. D **51**, 1125 (1995) [Erratum-*ibid.* D **55**, 5853 (1997)].
- [6] E. Braaten, S. Fleming, and T. C. Yuan, Ann. Rev. Nucl. Part. Sci. **46**, 197 (1996).
- [7] J. F. Amundson, O. J. P. Éboli, E. M. Gregores, and F. Halzen, Phys. Lett. B **372**, 127 (1996).
- [8] J. F. Amundson, O. J. P. Éboli, E. M. Gregores, and F. Halzen, Phys. Lett. B **390**, 323 (1997).
- [9] O. J. P. Éboli, E. M. Gregores, and F. Halzen, *Proceedings of the 26th International Symposium on Multiparticle Dynamics (ISMD 96)*, Faro, Portugal, 1996.
- [10] A. Edin, G. Ingelman, and J. Rathsmann, Phys. Rev. D **56**, 7317 (1997).
- [11] C. B. Mariotto, M. B. Gay Ducati, and G. Ingelman, Eur. Phys. J. C **23**, 527 (2002).
- [12] M. Kramer, Prog. Part. Nucl. Phys. **47**, 141 (2001).
- [13] G. A. Schuler and R. Vogt, Phys. Lett. B **387**, 181 (1996).
- [14] R. Gavai, D. Kharzeev, H. Satz, G. A. Schuler, K. Sridhar, and R. Vogt, Int. J. Mod. Phys. A **10**, 3043 (1995).
- [15] G. A. Schuler, arXiv:hep-ph/9403387.
- [16] O. J. P. Éboli, E. M. Gregores, and F. Halzen, Phys. Lett. B **395**, 113 (1997).
- [17] O. J. P. Éboli, E. M. Gregores, and F. Halzen, Phys. Rev. D **60**, 117501 (1999).
- [18] O. J. P. Éboli, E. M. Gregores, and F. Halzen, Phys. Lett. B **451**, 241 (1999).
- [19] O. J. P. Éboli, E. M. Gregores and F. Halzen, Phys. Rev. D **67**, 054002 (2003).
- [20] O. J. P. Éboli, E. M. Gregores, and F. Halzen, Phys. Rev. D **64**, 093015 (2001).
- [21] T. Stelzer and W. F. Long, Comput. Phys. Commun. **81**, 357 (1994).
- [22] H. Murayama, I. Watanabe, and K. Hagiwara, KEK-91-11.
- [23] G. P. Lepage, CLNS-80/447.

- [24] M. Gluck, E. Reya, and A. Vogt, Phys. Rev. D **46**, 1973 (1992); M. Gluck, E. Reya, and A. Vogt, Phys. Rev. D **45**, 3986 (1992).
- [25] M. Gluck, E. Reya, and M. Stratmann, Phys. Rev. D **51**, 3220 (1995).
- [26] M. Klasen, B. A. Kniehl, L. N. Mihaila, and M. Steinhauser, Phys. Rev. Lett. **89**, 032001 (2002).